Extreme Computing: Homework 2

Michael S. Emanuel, Jonathan Guillotte-Blouin, Yue Sun April 15, 2019

1 Problem 1: Channel Flow with a central narrowing

Simulating channel flow in 2D with a narrowing is the target.

The type of flow in absence of the narrowing is the well-known Hagen-Poiseuille flow (and by the way, Poiseuille was a physicist and physiologist who studied blood flows in a systematic way).

Let's write the corresponding grid for a straight channel aligned along, say, the x axis.

When constructing the grid and using it in the LBM context you should apply what you have learned about grid management.

Let's recall that in absence of open boundaries (inlet or outlet), each fluid node should always be surrounded by other fluid or wall nodes to preserve mass and momentum locally (no leakage rule).

The solution should employ two different options:

- 1. A periodic channel (aligned with the x direction): start from a quiescent fluid and apply a body acceleration uniformly through the fluid until you match the Reynolds number at steady state.
- 2. A non-periodic channel with inlet and outlet faces and by applying a uniform velocity at inlet and outlet with plug flow profiles.

Use no-slip boundary conditions at the walls and a Reynolds number of 10^{-2} computed from fluid velocity imposed at x = 0 (the inlet region for non-period channel) and characteristic length being H.

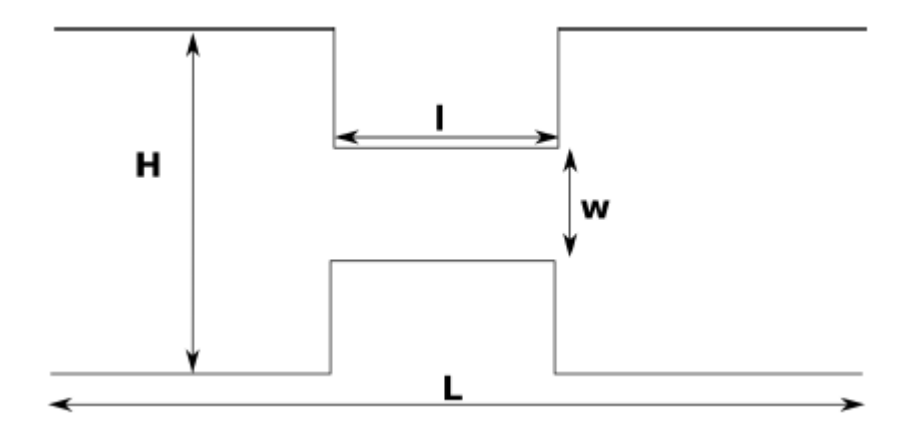


Figure 1: The geometry for the channel with central narrowing.

Solution

Our solution to this problem can be found in the folder hw2/lbm_7 in our team's repository for this course. Here is a brief overview of the components in our solution.

The file lattice.hh declares and implements the class lattice (that is, it's a header-only implementation). One instance of this class represents a single point on the lattice. It keeps track of populations f_0 through f_8 and their equilibrium values. It also tracks the hydrodynamic values ρ , u_x , u_y and p (pressure). The function hydro computes the hydrodynamic variables as a function of the populations. The function equilibrium computes the equilibrium populations as a function of the hydrodynamic macro quantities. The function collide does the post-collision update, relaxing each population towards the equilibrium. The parameter tau controls the rate of relaxation to equilibrium. As we learned in class, there is a linear relationship between τ and the kinematic viscosity ν , namely

$$\nu = \frac{2\tau - 1}{6}.$$

The files 1bm.hh and 1bm.cc declare and implement the class that builds the overall lattice Boltzmann grid. This class has member variables tracking the parameter values for the simulation, including the Reynolds Number Re, the relaxation time τ , the kinematic viscosity ν , and the length scale D. The number of grid points in the x and y directions are nx and ny. We use the strategy recommended by Sauro Succi and include buffers around the outside. We chose direct addressing rather than indirect addressing for this problem because the grid is rectilinear and dense. The biggest member variable is a pointer to an array of lattice objects, named f. There is also a Boolean array of obstacle indicators obs, which would be used as a flag to indicate whether this lattice is a fluid or a solid.

The initialization routines parallel the lattice class and Sauro's scheme, including initialize, init_hydro, init_flow, init_poiseuille and init_pop. The solver is methods include the following: solve, bc, pbc, mbc, stream, hydro, equilibrium, collide, force, obstacle, and set_channel. The post-processing methods are set_dir and output.

The driver programs are 1bm_pbc and pbm_mbc. These handle the periodic boundary condition (applying a body acceleration) and mixed boundary condition (applying a uniform velocity), respectively. There isn't too much happening in the driver programs; the heavy lifting is done in the lattice and 1bm classes. Each driver sets up the main problem instance, solves it, and writes the output. They then enter a loop where different widths w are simulated, for w in the range 10, 20, 30, 40, 50. In the periodic boundary driver 1bm_pbc only, we also have an additional loop over relaxation times τ in the range 0.65, 0.70, 0.75, 0.80, 0.85, 0.90, 0.95, 1.00. These correspond to kinematic viscosities in the range 0.05 to 0.1667 and address the last part of question 1.

Finally a good deal of post-processing is done in a Jupyter notebook called viz.ipynb. This started out limited to visualization, but we also compute some summary statistics asked for below. The common approach is to open a directory of frames containing one simulation run. Typically we use only the last frame, to answer questions about the end of the simulation which should be close to steady state.

In the Appendix A we provide a comparison between our LBM solver on the Poiseuille flow with analytical solution to prove the validity of our solver.

For a fixed set of values for the geometry as in Fig. 1, (suggested values L = 200, H = 60, l = 50, w = 30), calculate the following quantities:

- 1. The pressure field
- 2. The velocity field
- 3. The volume flow rate
- 4. The average and maximum velocities in the channel

Solution

The question specifically asks that we compute the pressure field, velocity field, volume flow rate, and the average and maximum velocities in the channel. Each frame includes entries at every grid point for the density ρ , the x-velocity u_x , the y-velocity u_y , and the pressure p. We compute the speed v in post-processing as $v = \sqrt{u_x^2 + y_y^2}$. We will present our results for the four fields as plots in the base case at end end of the simulation (frame 99). Note that the program outputs roughly every 100 frame. Set $Re = 0.01, \nu = 0.1$.

I. Periodic Channel In Appendix A we specify how to set the simulation constants. Our solver allows users input Re, τ and forcing to fix u_{max} and ν values. The lbm.cc has an inherent attribute which will do the calculation of nu, and the calculation of forcing is also provided in the driver file. For this particular visualization, we have

$$Re = 0.01 \tag{1}$$

$$\nu = \frac{2\tau - 1}{6} = 0.1 \Rightarrow \tau = 0.8 \tag{2}$$

$$u_{max} = \frac{ReD}{\nu} = \frac{1}{60000} \tag{3}$$

$$\mu = \rho \nu = 0.1 \tag{4}$$

$$force = \frac{8\mu u_{max}}{D^2} = 3.7e - 9 \tag{5}$$

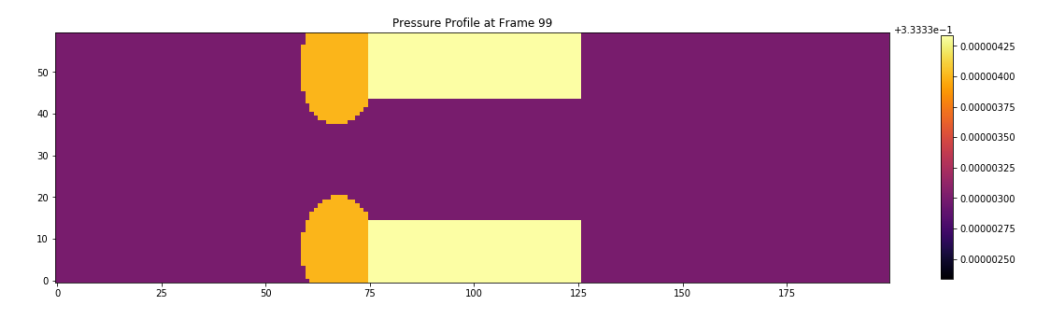


Figure 2: Pressure field of the periodic channel.

The pressure field is everywhere around 0.333, which is consistent with the mass conservation in the periodic case. We then compare the average pressure with the average density.

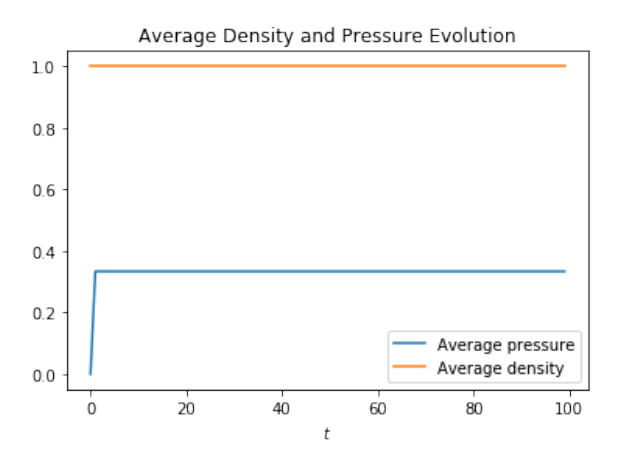


Figure 3: Time evolution of average density and average pressure.

Both density $(\rho = 1)$ and pressure $(p = \frac{1}{3})$ are conserved in this simulation, where the pressure value is approximately one-third of the density value. This coincides with the pressure-density relation in the setup:

$$p = c_s^2 \rho = \frac{\rho}{3}$$

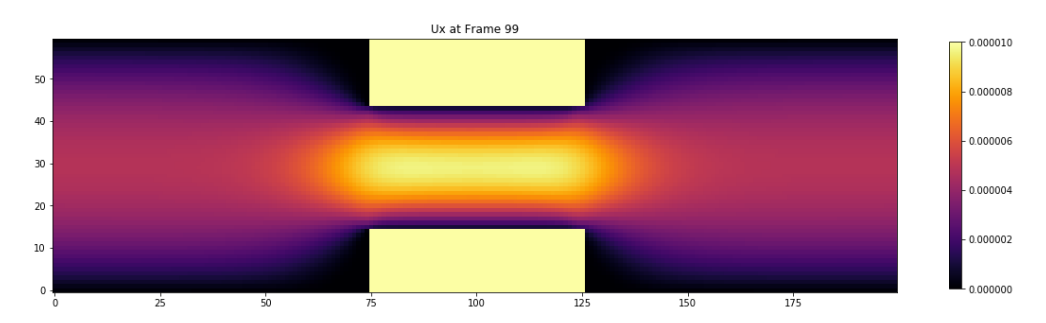


Figure 4: Velocity field in the x direction of the periodic channel.

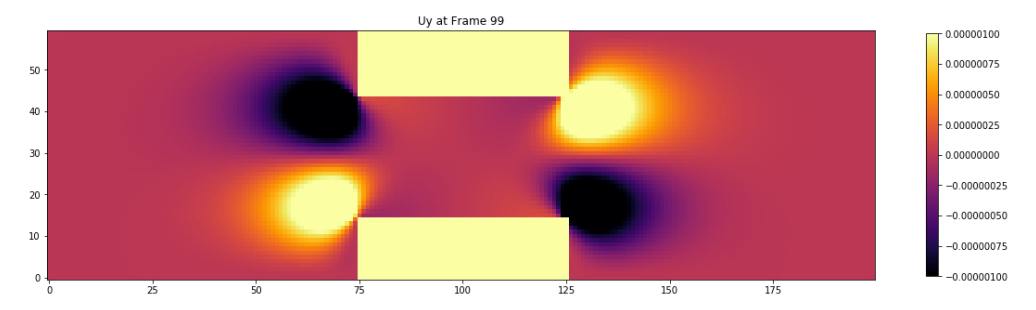


Figure 5: Velocity field in the y direction of the periodic channel.

We plot the velocity profile in both x and y direction along the y axis at $x = \frac{L}{2}$. Though encountering the narrowing, u_x starts from transient and still develops into a parabolic shape, whereas u_y is close to zero. This is consistent with the expected results of a periodic Poiseuille flow.

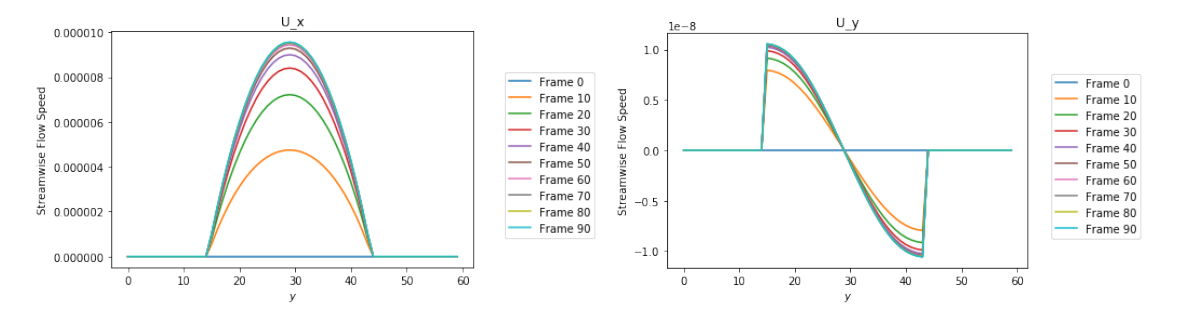


Figure 6: Time evolution of average density and average pressure.

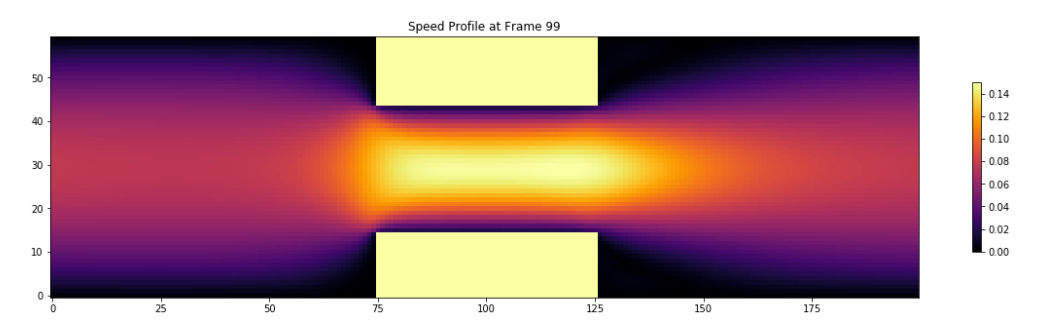


Figure 7: Velocity field of the periodic channel.

We can only compare the simulation results with the analytical solution of no narrowing. We use the last frame u_x at $x = \frac{L}{2}$ since the Poiseuille flow is steady. Though the narrowing restricts the parabolic shape to develop, near the centerline the u_x shows the parabolic shape that matches the analytical solution.

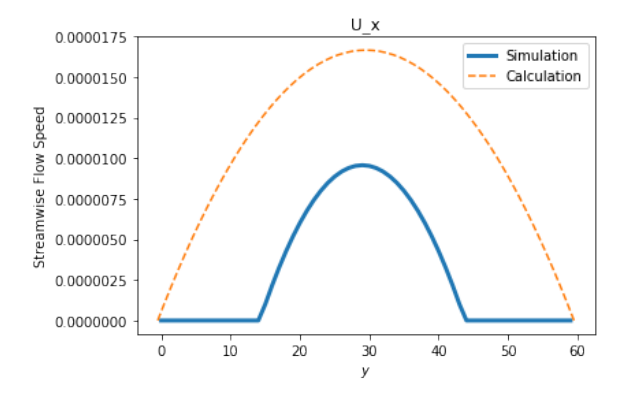


Figure 8: Simulation result vs. analytical solution of u_x .

We computed the speed v in the channel and the volume flow rate $Q = \int_0^H v \ dy$ as a post-

processing step in viz.ipynb. At the last iteration, we have

$$\overline{v} = 0.000003$$

 $\max(v) = 0.000010$
 $Q \approx 0.0001928$

The volume flow rate for steady state Poiseuille flow without the narrowing nor obstacle has the analytical form

$$Q = \frac{forceD^3}{12u} \approx 0.00066$$

which is roughly three times the simulated volume flow rate. This is consistent with the one-third relation in the average velocity and maximum velocity. We plot the average and maximum velocity, along with the volume flow rate with respect to time, and the three quantities develop into steady state as the simulation goes in.

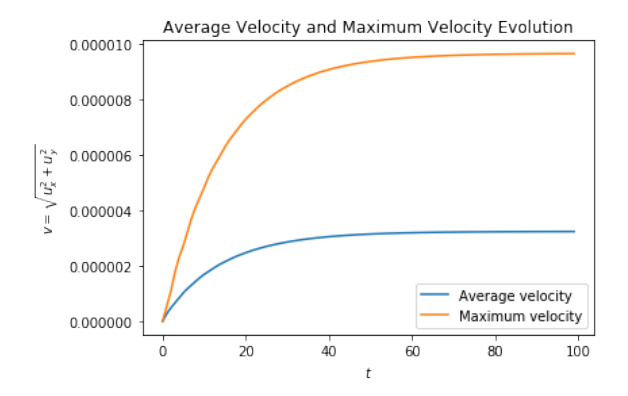


Figure 9: Time evolution of average velocity and maximum velocity.

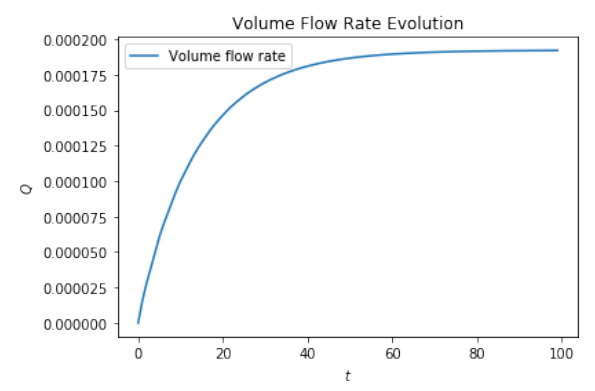


Figure 10: Time evolution of volume flow rate.

II. Non-Periodic Channel In the periodic case we fix the forcing term to introduce acceleration uniformly through the fluid. For the non-periodic case, we have an inlet and an outlet. By applying a uniform velocity at inlet and outlet with plug flow profiles, the flow will gradually become a steady Poiseuille flow because plug flow implies pressure gradient. For this particular visualization, we have

$$Re = 0.01 \tag{6}$$

$$\nu = \frac{2\tau - 1}{6} = 0.1 \Rightarrow \tau = 0.8 \tag{7}$$

$$u_{max} = \frac{ReD}{\nu} = \frac{1}{60000} \tag{8}$$

$$\mu = \rho \nu = 0.1 \tag{9}$$

$$\mu = \rho \nu = 0.1$$
 (9)

$$\frac{dp}{dx} = \frac{8\mu u_{max}}{D^2} = 3.7e - 9 \text{ (not used)}$$
 (10)

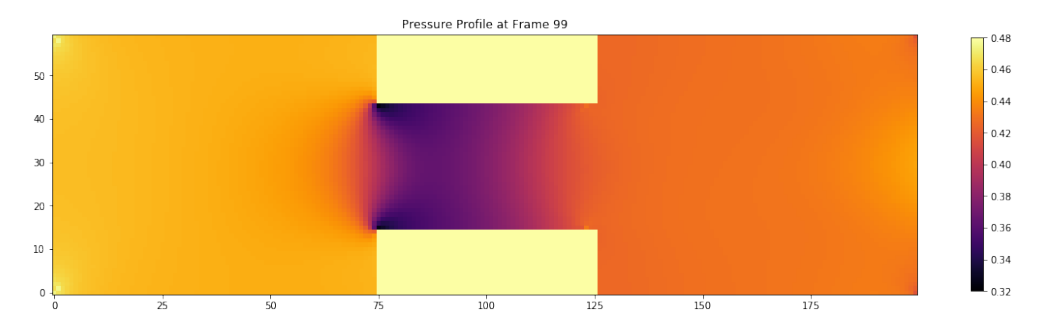


Figure 11: Pressure field of the non-periodic channel.

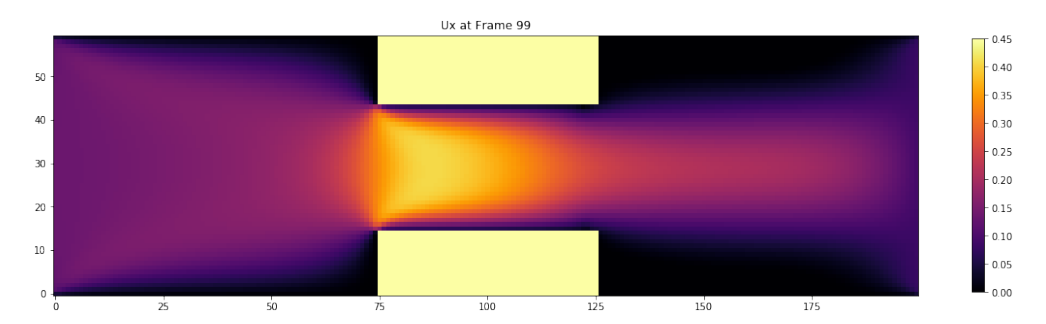


Figure 12: Velocity field in the x direction of the non-periodic channel.

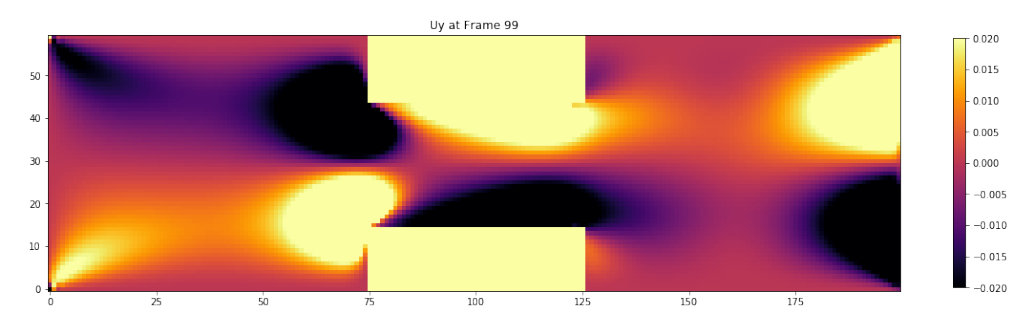


Figure 13: Velocity field in the y direction of the non-periodic channel.

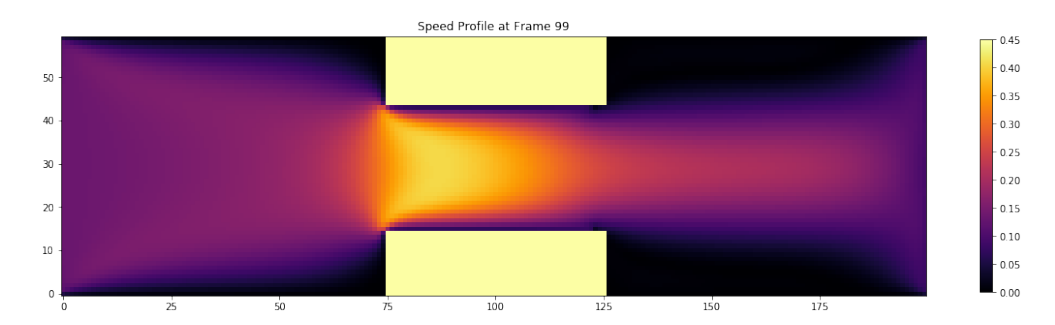


Figure 14: Velocity field of the non-periodic channel.

We computed the speed v in the channel and the volume flow rate $Q = \int_0^H v \, dy$ as a post-processing step in viz.ipynb. At the last iteration, we have

$$\overline{v} = 0.118941$$

$$\max(v) = 0.407619$$

$$Q \approx 8.861476$$

We plot the average and maximum velocity, along with the volume flow rate with respect to time, and the three quantities develop into steady state as the simulation goes in.

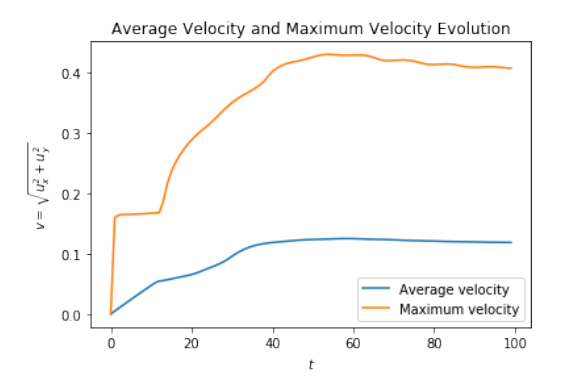


Figure 15: Time evolution of average velocity and maximum velocity.

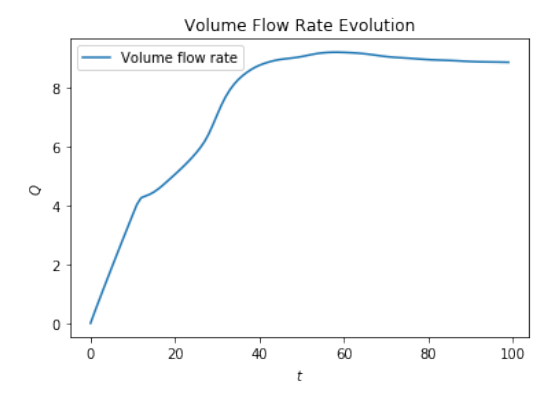


Figure 16: Time evolution of volume flow rate.

We computed the volume flow rate as the amount of fluid passing a vertical line at a given value of x. We would expect that this would be equal for any x we chose at steady state by conservation of mass. This is close to being true. We therefore chose to take the mean of this quantity across all the x values in our grid to get the most accurate estimate of the volume flow. As a sanity check, we printed out the volume flow every 20 steps from x = 0 to x = 200. The results were all within 0.02 of the mean, except for the point at x-100 in the middle of the inlet, where it was 0.08 below the mean.

Here are a few comments about these plots. There is a significant difference in the scale of the speed and volume flow rate between the periodic and non-periodic cases. We have double checked our work and believe it to be correct. The problem statement is in terms of a target Reynolds number, and the way we are calibrating the fluid speeds to achieve this is quite different between the two cases. We have confidence that each simulation is correct as presented.

The overall pressure profile is encouraging. The pressure varies only very slightly, as we expect for an incompressible fluid simulation. The variations make sense too, as the modeled pressure is slightly higher on the left and lower on the right. The profile of the x-velocity u_x is intuitive; the fluid needs to speed up considerably in the narrowing for the flow to conserve mass. We can also see it slowing down next to the boundary due to the no-slip boundary condition. The y-velocity pattern shows very little flow in the y direction, with four small pockets next to the four corners where the fluid needs to narrow then widen out to pass through the narrow channel. Overall these results make sense and look good to us. Finally, we did a comparison of these results against the analytical results for the PBC and found a good agreement.

Repeat the simulation by varying the width of the narrowing w.

Plot: Show how the flow rate changes by varying w in the range 0 < w < 50

Compare the pressure at the narrowing with the simple Bernoulli estimate for inviscid flows, stating that

$$\frac{1}{2}\rho u_o^2 + p_o = \frac{1}{2}\rho u_i^2 + p_i$$

where u_o and p_o are cross-sectional averages of velocity and pressure at x = 0 for a periodic system or at the inlet otherwise, and u_i and p_i are the same quantities at the center of the narrowing.

Solution

We simulated w values at 10, 20, 30, 40 and 50. Towards the bottom of viz.ipynb, we have a small function that computes the volume flow rate for a simulation as described above. We use it to assemble the volume flows for these widths in both the periodic and non-periodic boundary conditions. Here are the requested plots:

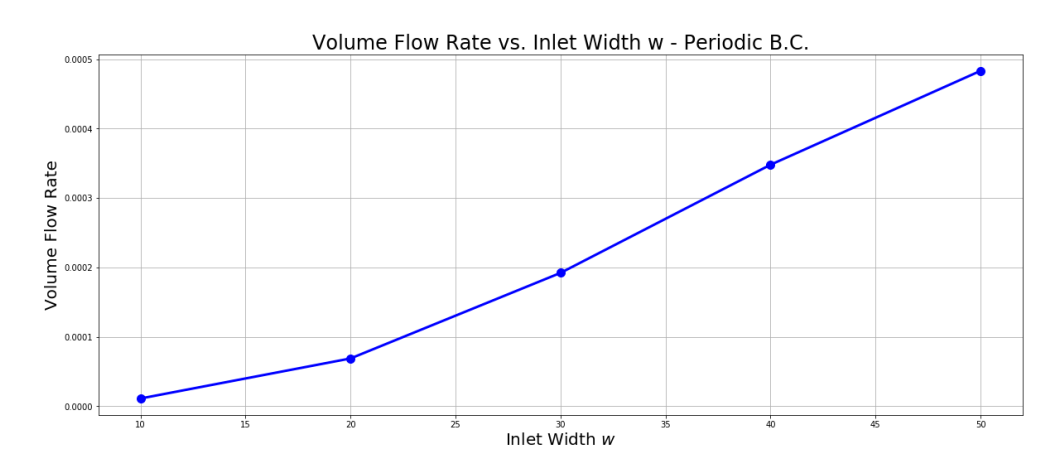


Figure 17: Flow vs. Channel Width w of the periodic channel.

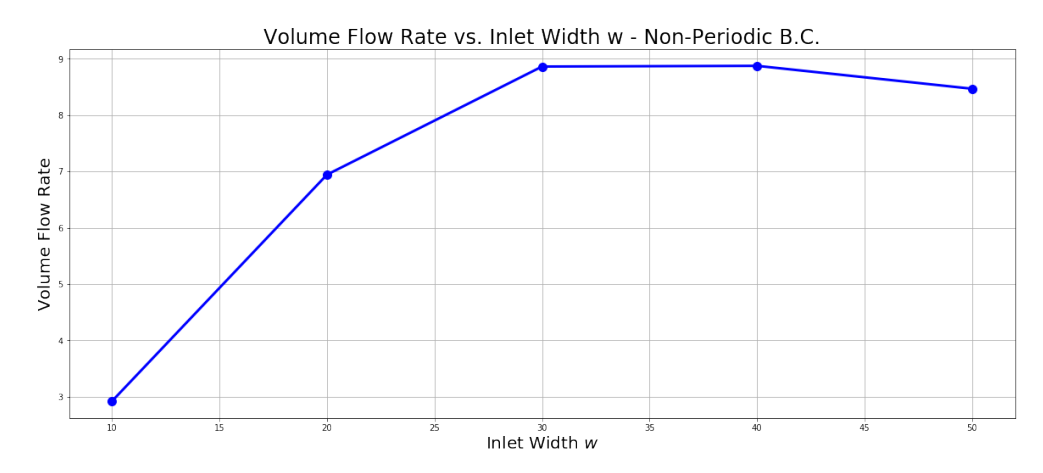


Figure 18: Flow vs. Channel Width w of the non-periodic channel.

As expected, we see that the volume flow rate increases for the periodic case with a roughly parabolic shape. The flow rate also increases for the non-periodic case, but plateaus past a width of 30. However, we need to be very careful with our intuition here, because we've standardized on a Reynolds number of 0.01 rather than a pressure gradient. Our intuition about how the flow depends on the width of the opening is based on varying the width while holding the pressure gradient constant. This simulation isn't calibrated that way, so it's measuring something slightly different, especially in the non-periodic case.

Plot: Plot the obtained pressure vs the Bernoulli estimate by varying the LBM kinematic viscosity in the range 0.05 : 0.1667.

Solution

We calculate this for the periodic flow case in the next section of viz.ipynb. We begin by computing both sides of the Bernoulli relationship in the base case as a sanity check for the method. Using the quantities p_0 , and u_0 at x = 0 (start of the channel) we find an energy density of 0.339. Using the quantities p_i and u_i at x = 100 (center of the channel) we find an

energy density of 0.334. Since we expect these to be approximately equal, it's encouraging that they are this close together. In the Python function calc_pressure_narrow we calculate the pressure p_i that would be implied at the narrowest point of the channel by solving this relationship for p_i in terms of p_0 , u_0 and u_1 .

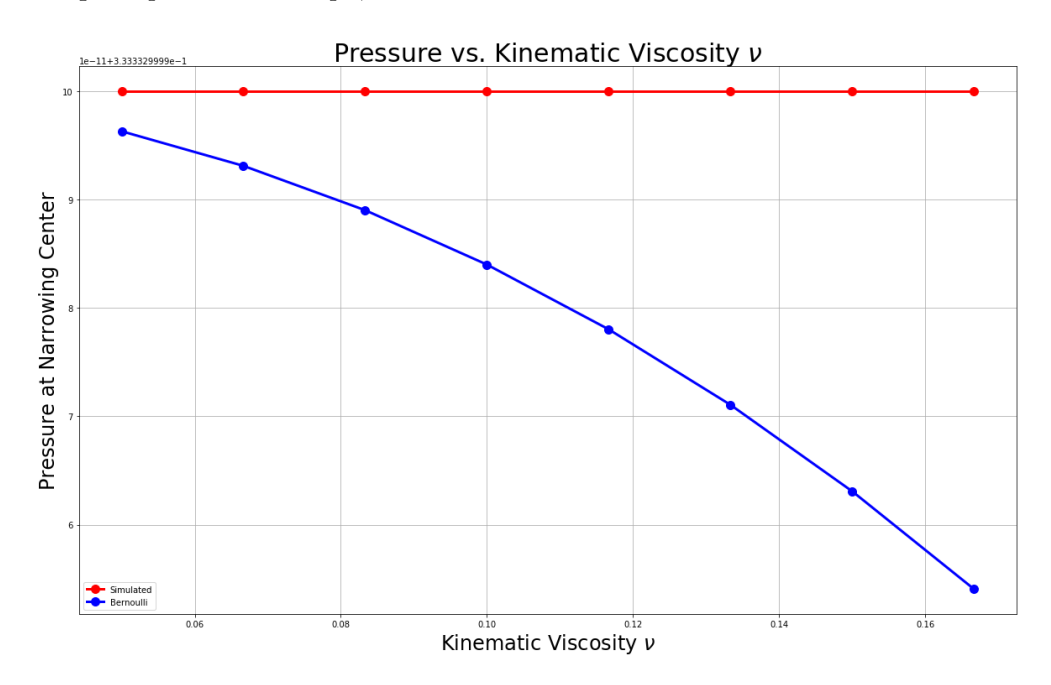


Figure 19: Pressure vs. the Bernoulli estimate of the periodic channel.

The scale on this plot is very compressed, so it's important not to overreact to the shape of the curves being different. The high level story here is the pressure scale ranges from 0.326 to 0.336, so the two methods are actually in quite good agreement over this range of viscosities. One thing the chart does seem to be suggesting is that that the Bernoulli approximation is breaking down at an accelerating rate as the viscosity drops in the range of 0.05. This isn't too surprising, when we recall that it's an "inviscid" approximation. That approximation will be more accurate at higher viscosities.

2 Problem 2: Basic CUDA and GPUs

This problem was submitted by Dan Willen daniel.p.willen@gmail.com

Consider the equation

$$\frac{\partial u}{\partial t} = D\nabla^2 u,\tag{11}$$

on the domain $0 \le x, y \le \pi$, with u = u(x, y, t), D the diffusive constant, and ∇^2 the Laplace operator. The boundary conditions are of the homogeneous Dirichlet type:

$$u(x = 0, y) = u(x = \pi, y) = u(x, y = 0) = u(x, y = \pi) = 0,$$
(12)

and the initial condition is

$$u(x, y, t = 0) = \sin(x)\sin(y). \tag{13}$$

The solution to this equation is

$$u(x, y, t) = \sin(x)\sin(y)\exp(-2Dt) \tag{14}$$

Using a second-order central difference in space and first order forward difference in time, the discretization of (11) is

$$u_{i,j}^{(n+1)} = u_{i,j}^{(n)} + \frac{D\Delta t}{\Delta x^2} \left[u_{i+1,j}^{(n)} + u_{i-1,j}^{(n)} + u_{i,j+1}^{(n)} + u_{i,j-1}^{(n)} - 4u_{i,j}^{(n)} \right], \tag{15}$$

where $u_{i,j}^{(n)}$ is the value of u at the n^{th} time step at grid point (i,j), $\Delta t = \Delta x^2/4D$ is the time step size, and Δx is the grid spacing in the x and y directions.

- 1. Using Cuda, solve the discretized equations up to a time $t = \pi^2/D$ using the Jacobi method. A skeleton code is provided to assist you, with comments in the locations you should make changes.
 - Step I Declare, allocate, and initialize memory for the field variable ${\tt u}$ on the CPU. You should allocate enough memory for the grid, which has size $nx \times ny$ and initialize ${\tt u}$ to the initial condition. Make sure you free the memory at the end of the program.
 - Step II Declare and allocate the GPU memory for _u, _u_new and _error. Copy the CPU memory to the GPU; the other two arrays have been initialized to zero for you. Make sure you free the memory at the end of the program.
 - Step III Set up the kernel execution configuration for the GPU kernel based on the input domain size and the maximum threads per dimension, which is set at the top of the file as a #define. You will need to determine the number of threads per block and the number of blocks in each direction, as well as set up the dim3 variables.
 - Step IV Write a GPU kernel that advances to the next timestep using the Jacobi method. This should be done in parallel, not in serial.
 - Step V Write a GPU kernel that calculates the error between the numerical and analytic solutions at each point. Be careful to compare solutions at the correct timestep $\underline{\mathtt{u}}$ -new is at $t=(n+1)\Delta t$ and $\underline{\mathtt{u}}$ is at $t=n\Delta t$. Using this result, a parallel reduction using the Thrust parallel algorithms library has been provided to calculate the total error in order to find the average percent error at each grid point.

Step VI – At the end of the loop, copy the data back to the CPU.

Your program should take as an input the number of grid cells on one side of the domain. This has been set up for you such that the program can be run from the command line like:

```
./jacobi_solver.cu n
```

where $nx = ny = \mathbf{n}$ is the size of one side of the square domain. The program should output the percent difference between your result and the analytic solution, averaged over all of the grid nodes:

$$\epsilon = \frac{1}{n_x n_y} \sum_{i=1}^{n_x} \sum_{j=1}^{n_y} \frac{u_{i,j}^{(n)} - U_{i,j}^{(n)}}{U_{i,j}^{(n)}},\tag{16}$$

where U is the analytic solution.

Solution

Our solution to this problem can be found in the folder hw2/jacobi in our team's repository for this course. Here is a brief overview. There is only one source code file in this solution, parallel.cu, plus a short Makefile. We will say a few words about the six steps described in the algorithm overview.

In step 1, we declare, allocate and initialize memory for the field u on the CPU. This is done with the array u of size $nx \times ny$. It's a standard nested for loop over i and j, with the action happening in this statement:

```
u[j*nx + i] = sin(i * dx) * sin(j * dy);
```

In step 2, we allocate GPU memory for _u, _u_new, and _error. These are, respectively, the current field; the field at the next time step; and the error vs. the analytical solution. These two statements give an idea of how we allocate memory on the GPU and set it from the CPU:

```
cudaMalloc(&_u, nx*ny * sizeof(double));
cudaMemcpy(_u, u, nx*ny * sizeof(double), cudaMemcpyHostToDevice);
```

In step 3, we configure the GPU kernel, i.e. block sizes. The variables tx and ty and both set to the preprocessor constant MAX_THREADS_DIM. This is currently set to 16, but is hardware dependent and could change if we compiled on different hardware. A more sophisticated technique would be to detect the hardware and tune it accordingly, but we don't yet know how to do that, and it's not critical to performance here. Once the thread counts are set, the box sizes bx and by are a straightforward calculation where we perform integer division rounding up. Then we create dim3 structures. These two statements give the flavor:

```
int bx = (int) ceil((double) nx / tx);
dim3 dimBlocks(tx, ty);
```

In step 4, we write the GPU kernel that advances the simulation one time step. This is really the heart of the program. At the top, we compute the two indices ti and tj from the properties of the block. We compute the updated value $U_{i,j}^{n+1}$ as the old value $U_{i,j}^n$ plus a prefactor $\frac{D\Delta T}{\Delta x^2}$ multiplied by a finite difference stencil for the second derivative. This statement computes the right hand term, i.e. the prefactor times the second derivative:

```
double rightTerm = pref * (_u[tj*nx + (ti+1)] + _u[tj*nx + (ti-1)] + _u[(tj+1)*nx + ti] +_u[(tj-1)*nx + ti] -4*_u[tj*nx + ti]);
```

This statement is wrapped inside an if and only executes when ti and tj are both in the range mapping to actual data points. This check is necessary in case the number of grid points nx and ny are not integer multiplies of the thread count.

In step 5, we write the GPU kernel to compute the error against the analytical solution. It's a similar for loop to step 4, with the expected statements inside it. We compute the numerical and analytical solutions, then set the error equal to the absolute value of their difference:

```
double discretizedValue = _u[tj*nx + ti];
double analyticalValue = sin(dx * ti)*sin(dy * tj)*exp(-2*D*t);
_error[tj*nx + ti] = abs(discretizedValue - analyticalValue);
Step 6, copying back to the CPU, is a one liner:
```

```
cudaMemcpy(u, _u, nx*ny * sizeof(double), cudaMemcpyDeviceToHost);
```

We ran this program on grid sizes that were powers of 2 in a reasonable range. Specifically, we ran this for n in 16, 32, 64, 256, 512. All runs were done on a PC with a high end Titan V GPU. We assembled charts and regression fits in <code>jacobi.ipynb</code>. We present the highlight below.

If you have time, discuss the following:

• How does the error change as you increase the resolution? Does this behavior make sense?

Solution

The error scales according to ΔX^2 . We ran a linear regression of $\log(\epsilon) \sim \log(n)$ and the estimated slope was -1.997, very close to theoretical value of -2.0 we would have expected. Here is the plot:

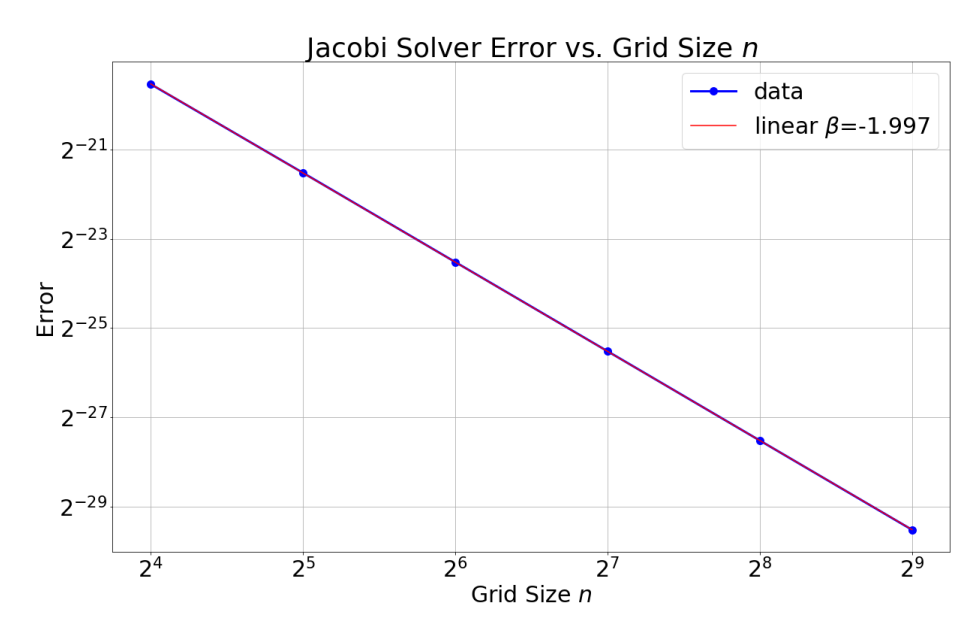


Figure 20: Jacobi error vs. grid size.

• How does the runtime scale with the resolution? You can get a rough estimate by using the bash command time when executing your program, like:

./jacobi_solver.cu n

and using the result for real.

Solution

Intuitively we would expect that the run-time should scale quadratically with the grid size. This result is borne out over the range of n tested above. The numerical estimate of the slope of $\log(t)$ vs. $\log(n)$ was 1.922. Here is the plot:

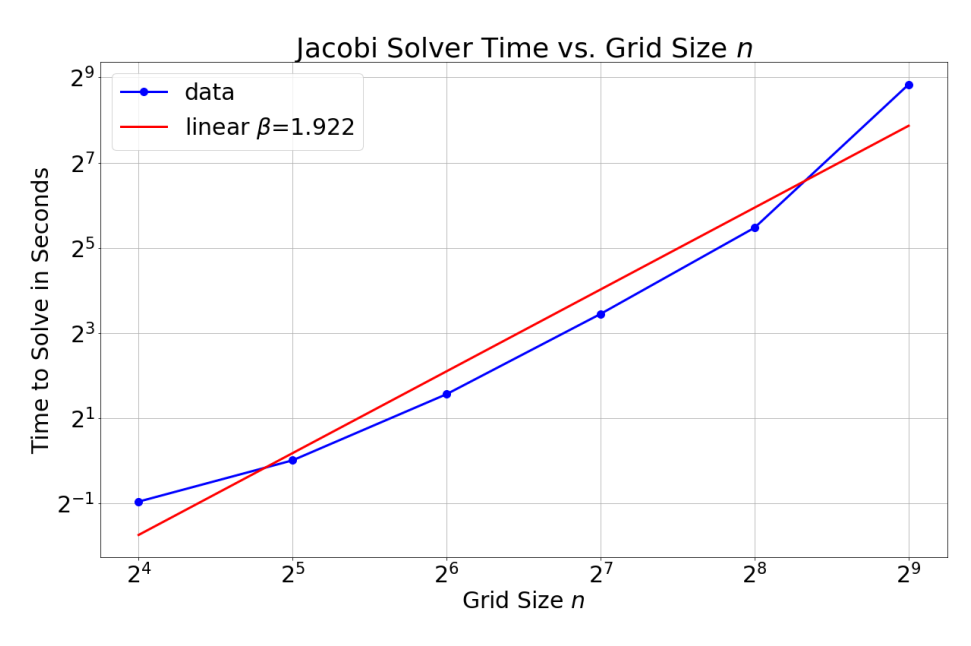


Figure 21: Jacobi runtime vs. grid size.

 How does the runtime change as you change the kernel execution configuration? e.g., play around the MAX_THREADS_DIM parameter as well as different schemes for setting up the thread blocks.

Solution

We tried the following choices for the number of threads: 8, 16, 32, 64. 64 threads didn't run; the program terminated immediately. Run-time with 8, 16, and 32 was 39.940, 44,363, and 36.698 seconds, respectively. This didn't make a huge amount of sense, because it wasn't even monotonic. A second trial with n=16 took 40.542 seconds. If we had to guess, there is probably an advantage to using as many threads as possible (probably 32 on the Titan-V card), but this advantage likely matters more for larger calculations than this one for n=256.

• Use shared memory in the Jacobi kernel

A Validity of the LBM solver

First we verify the periodic version. We follow the same setup of a simple Poiseuille flow in Sauro Succi's The Lattice Boltzmann Equation for Fluid Dynamics and Beyond in Section 7.3 (page 103), with no channel narrowing or obstacle: $L = 128, H = 32, \nu = 0.1, u_{max} = 0.1$. Note that our solver set Re to fix u_{max} , set τ to fix ν , and set the characteristic length D = H. (This u_{max} is not to set the initial velocity as u_{max} , but the steady state velocity which can fix Re.) In order to get the steady state velocity to be equal to $u_{max} = 0.1$, we fix the Reynolds number Re, the relaxation time τ and the forcing term by

$$\tau = \frac{6\nu + 1}{2} = 0.8\tag{17}$$

$$Re = \frac{u_{max}L}{\nu} = 32\tag{18}$$

$$force = \frac{8\mu u_{max}}{H^2} = \frac{8\rho\nu u_{max}}{H^2} = \frac{1}{12800}$$
 (19)

We set the initial density, velocity in both directions to be 1, 0, 0, run the simulation 10000 iterations and output every 100 frames. We plot the velocity fields at the center of the channel $(x = \frac{L}{2})$

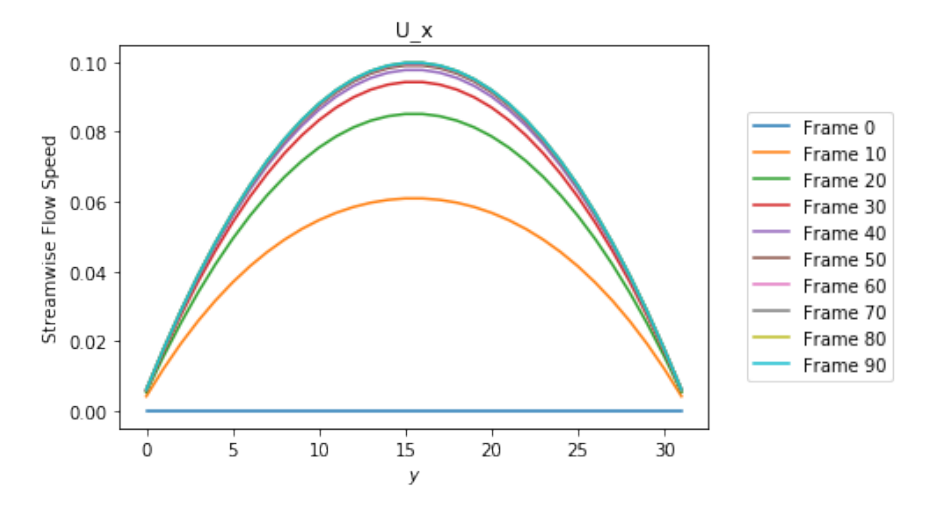


Figure 22: U_x profile of Poiseuille flow in a periodic channel.

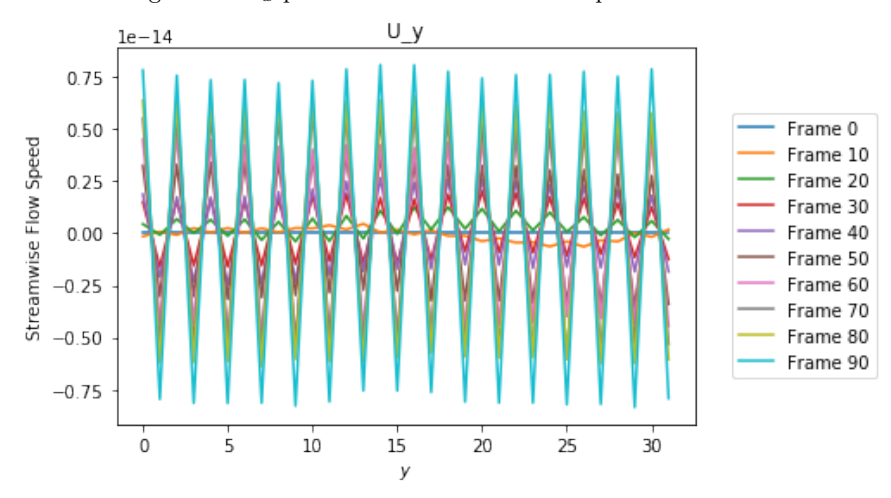


Figure 23: U_y profile of Poiseuille flow in a periodic channel.

The velocity in the x direction u_x starts from zero, gradually develops into a parabolic shape in the vertical direction, reaches the steady state velocity $u_{max} = 0.1$ and stays at the speed. The velocity in the y direction u_y experiences some oscillation, but remains at almost zero. Next We plot the average density at each output frame to verify conservation of mass.

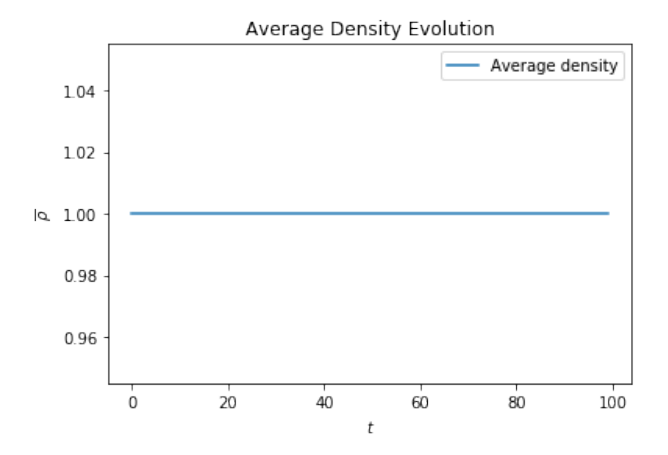


Figure 24: Time evolution of average density.

The horizontal line verifies matches the expectation that density of the Poiseuille flow in a periodic channel is conserved, u_x will have a parabolic shape and u_y is zero. Last we compare the simulation result of u_x with analytical solution

$$u(y) = \frac{force}{2\mu}y(H - y)$$

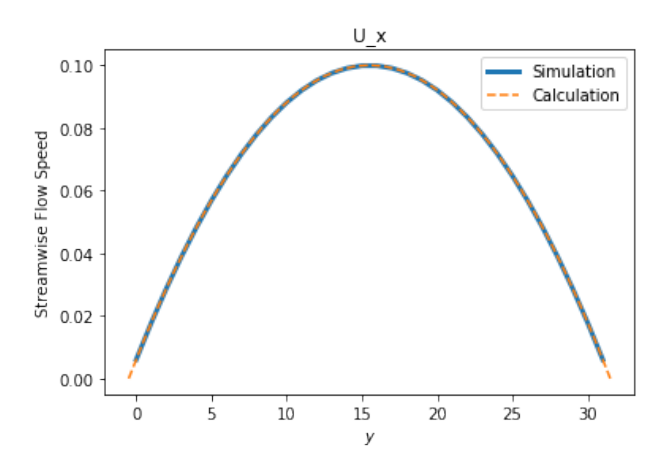


Figure 25: Simulation result vs. analytical solution of u_x .

The simulation u_x is chosen to be of the last frame, where the Poiseuille flow has reached steady state. And we can see the simulation result matches exactly with the analytical solution.

Second we verify the open boundary version with the same setup as in the periodic version. Note that for the west inlet and east outlet we impose a different boundary condition. We drive the flow with a given velocity at the inlet, not imposing a pressure difference manually at the start. We assign a given velocity profile $u_{in}(y)$ at the inlet. For the outlet we choose to impose a no-flux condition, i.e. $\partial_n u = 0$ to minimize the risk of backward propagating disturbance if $\frac{L}{W}$ is not large enough. Set $u_{max} = 0$, $\nu = 0$, the simulation constants are

$$\tau = \frac{6\nu + 1}{2} = 0.8\tag{20}$$

$$Re = \frac{u_{max}L}{\nu} = 32\tag{21}$$

$$\frac{\Delta p}{\Delta x} = \frac{8\mu u_{max}}{H^2} = \frac{8\rho\nu u_{max}}{H^2} = \frac{1}{12800} \tag{22}$$

$$\Delta \rho = 3\Delta p = \frac{8\mu u_{max}L}{H^2} = 0.03 \tag{23}$$

We set a uniform velocity $u_{in} = \frac{Re\nu}{D} = 0.1$, run 2000 iterations and output every 20 frames. We plot the corresponding figures at $x = \frac{L}{2}$. Note that although u_x develops into parabolic shape and stays at the steady state velocity, it does not match the shape of the calculated velocity. Because we impose a plug flow, not actually imposed a density difference in the flow. The velocity at the y direction is not close to zero as in the periodic case, which falls within the expectation that since there is flow coming in uniformly, the motion of the flow should include some y directional movement.

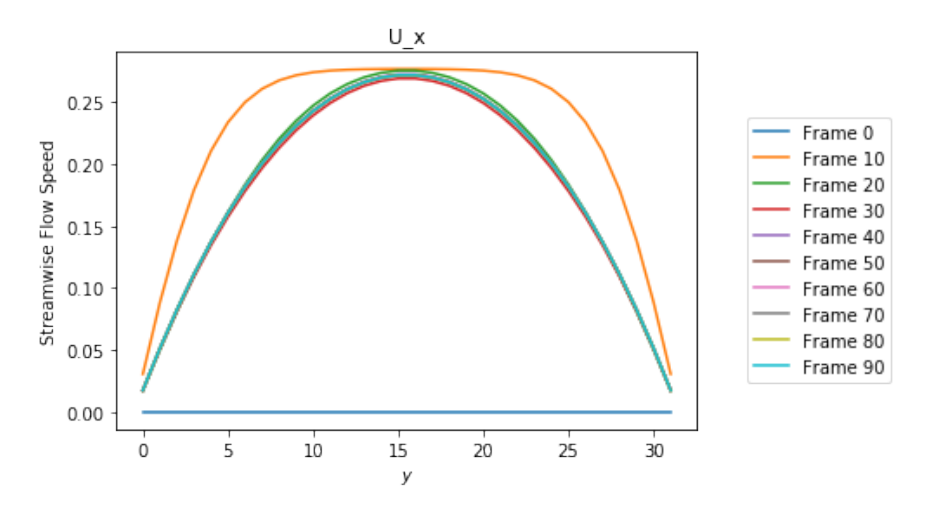


Figure 26: U_x profile of Poiseuille flow in an open channel with plug flow input.

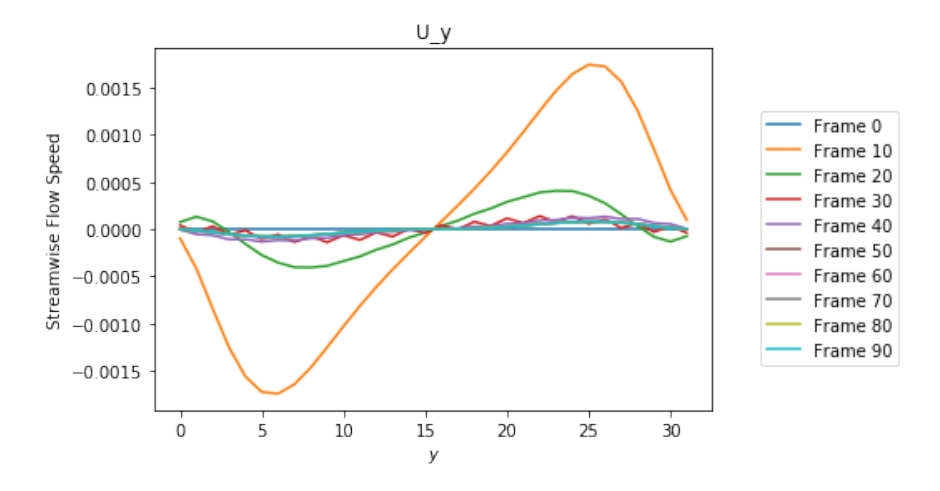


Figure 27: U_y profile of Poiseuille flow in an open channel with plug flow input.

We also compare the density and pressure evolution. Since there is not pressure/density gradient imposed in the system, the density stays at constant. The pressure starts from zero, and gradually develops into its steady state. Note that although the pressure is slightly higher in the steady state as in the periodic case, it still follows the one-third relation with the density.

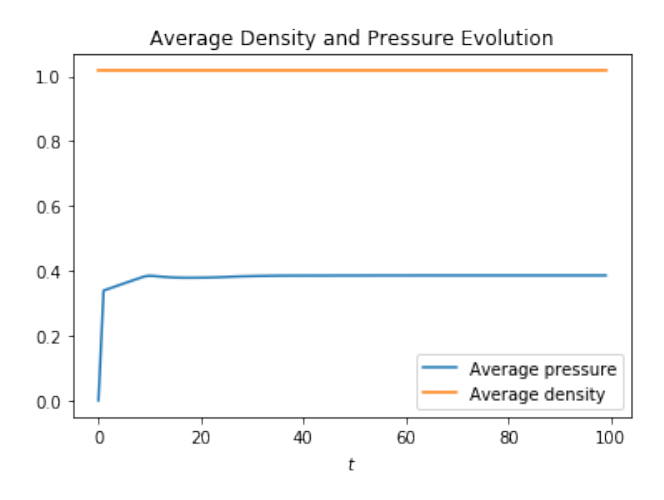


Figure 28: U_y profile of Poiseuille flow in an open channel with plug flow input.